

© 2019 Christopher G. Sain

AN OPENDSS IMPLEMENTATION OF A GENERIC MUNICIPAL
MICROGRID FOR CO-SIMULATION

BY

CHRISTOPHER G. SAIN

THESIS

Submitted in partial fulfillment of the requirements
for the degree of Master of Science in Electrical and Computer Engineering
in the Graduate College of the
University of Illinois at Urbana-Champaign, 2019

Urbana, Illinois

Adviser:

Professor Peter W. Sauer

ABSTRACT

This thesis provides a summary of the development process of a microgrid simulation model using OpenDSS software, as well as simulations and co-simulations using said model. Many power system research problems may be solved via the deployment simulations. However, for real-world problems the computational efforts for detailed dynamic modeling may be impractical or excessive. OpenDSS provides a framework within which a model of a small- or large-scale system may be implemented without the representation dynamics, with extensive co-simulation capabilities. We discuss the modeling of a generic 8-bus microgrid that consists of 200 residential loads plus an additional load for the local control building, three generation resources – solar, wind, and gas – and a battery storage resource. We use historical environmental data from Decatur, Illinois, together with realistic consumer load shapes to simulate and analyze various unbalanced and quasi-balanced situations. In addition, we present results of co-simulation studies on such a model in an OpenDSS application to evaluate various potential scenarios.

For Booster, my most loyal friend.

ACKNOWLEDGMENTS

I would like to thank my advisor, Professor Peter W. Sauer, for his guidance, support, and wealth of knowledge over the course of my master's study. I would also like to thank Professor Alejandro D. Domínguez-García and the members of the ARPA-E NODES group for their assistance and dedication during my time working with them. Finally, I would like to thank all my family and friends who helped and supported me along the way.

TABLE OF CONTENTS

LIST OF TABLES	vi
LIST OF FIGURES	vii
LIST OF ABBREVIATIONS	viii
CHAPTER 1 INTRODUCTION	1
1.1 Literature Survey	2
CHAPTER 2 THE MICROGRID	4
2.1 One-Line Representation	4
2.2 Generators and Storage	6
2.3 Transformers	6
CHAPTER 3 MODELING IN OPENDSS	8
3.1 Buses	8
3.2 Lines	8
3.3 Initial Simplified Model	9
3.4 Refined Model	11
3.5 Auxiliary Implementation of Dynamics	20
CHAPTER 4 AN APPLICATION IN DISTRIBUTED CONTROL STUDIES	24
4.1 Co-simulation Goals	24
4.2 Microgrid Model	25
4.3 Simulation	25
CHAPTER 5 CONCLUSIONS AND FUTURE WORK	31
REFERENCES	33

LIST OF TABLES

2.1	DER Parameters	6
2.2	Transformer Parameters	7
3.1	Buses in Network	8
3.2	Distribution Line Parameters	9

LIST OF FIGURES

2.1	One-line diagram of the microgrid to be modeled	5
3.1	Real power generated in preliminary test	10
3.2	Tie line voltage in preliminary test	11
3.3	Inverter efficiency curve	12
3.4	Historical solar data, Decatur, IL, 07/21/2017	13
3.5	Historical wind data, Decatur, IL, 07/21/2017	14
3.6	Generated load shapes	15
3.7	Combined neighborhood load, per phase	16
3.8	Simulated generation, full day	17
3.9	Simulated power exchanged on tie-line, full day	17
3.10	Simulated voltage on tie-line, full day	18
3.11	Simulated voltage on neighborhood bus, full day	18
3.12	Artificially inflated loads	19
3.13	Neighborhood voltage response to artificially inflated loads	20
3.14	Generator dynamic test	22
3.15	Dynamic tie-line exchange	22
4.1	System architecture for C-HIL co-simulation	27
4.2	Simulation results for “stepped ramp” input signal	28
4.3	Simulation results for first 5 minutes of PJM RegD signal	29
4.4	Simulation results for second 5 minutes of PJM RegD signal	30

LIST OF ABBREVIATIONS

ADN	Active Distribution Network
DER	Distributed Energy Resource
EPRI	Electric Power Research Institute
HIL	Hardware in-the-Loop
ISO	Independent System Operator
PQ	Active and Reactive Power
PV	Power and Voltage
RTO	Regional Transmission Organization
TAC	Technology Applications Center
TCUL	Tap Change under Load
UCSD	University of California, San Diego
UIUC	University of Illinois at Urbana-Champaign

CHAPTER 1

INTRODUCTION

When simulating power systems for research applications, often there arises the need for simulation tools that are not necessarily in the scope of the problem. For example, when attempting to test a system's response to a control algorithm, the researcher requires a system on which to apply the control scheme. It would be valuable to have a system model already created that was made available for such purposes. The topic of this thesis is to create such a model.

In particular, the goal is to create a “plug-and-play” model of a microgrid which may be used to test the efficacy of control algorithms under development. Because of the close ties between the University of Illinois at Urbana-Champaign (UIUC) and Ameren Illinois, the microgrid to be modeled is based upon Ameren's Technology Applications Center (TAC) microgrid [1], located next to the university. This model will be used by the NODES group in the Power and Energy Systems area at UIUC, in support of ongoing research into distributed control algorithms for distributed energy resources (DERs).

The simulation framework chosen for this model is OpenDSS, developed by the Electric Power Research Institute (EPRI). This software was chosen for several reasons.

1. It is free and open source, making the model easily transferred, modified, and updated as needed.
2. It has extensive co-simulation capabilities through its COM server, allowing for a driver program to run the simulation from almost any programming language/environment [2]. The driver used in this thesis is MATLAB.
3. It handles the simulation of both balanced and unbalanced networks.

4. It does not implement full dynamic modeling natively, allowing for a lighter load on computation resources and fast solution convergence.
5. It is widely used in industry for simulation of large and small scale networks, yielding comprehensive support documentation [2].

Rather than implementing a full dynamic model of a power system, which is often infeasible or unnecessary, the system may be modeled in OpenDSS, allowing for fast simulation yielding the steady-state response of the system to inputs. However, if dynamic response is desired, they may be added piecewise to the model via the driver program. This allows any critical dynamic performance to be modeled, while not requiring the entire network to be simulated as such. If desired, complete system dynamics could be added to the simulation [3].

This thesis is organized in the following manner. Chapter 1 outlines and motivates the problem to be solved, with a survey of contemporary research being performed in this area. Chapter 2 provides an in-depth definition of the microgrid: the nature of its network and topology, as well as power conversion and delivery elements. Chapter 3 summarizes the process of developing the model of such a microgrid using OpenDSS and preliminary simulations of its behavior. Lastly, Chapter 4 presents the results of an application for this simulation framework, using a similar microgrid model in co-simulation with a distributed control architecture currently under development at UIUC.

1.1 Literature Survey

Applications of open-source modeling are widespread, from industry supervisory control and data acquisition (SCADA) systems to university research. The most abundant literature concerns modeling of photovoltaic systems for impact studies. The authors of [4] seek to use OpenDSS to supplement existing models for a hybrid time-and-frequency domain simulation of the implementation of such photovoltaics on a large scale in an urban setting. They have chosen OpenDSS because many such hybrid simulations have been performed on the transmission level, rather than distribution.

Other applications of OpenDSS include interconnection studies [5], real-time simulation [6], and voltage control [7]. These papers focus on the ef-

fects of high-penetration levels of photovoltaics into the grid, and how they can cause problematic voltage conditions around the interconnections. The models attempt to take into account variations of residential and commercial loads and how different control schemes may assist in mitigating the over/undervoltage events at the interconnections. This includes Volt/VAR and Volt/Watt control, as well as the introduction of battery storage units into the network.

The authors of [6] describe their use of OpenDSS in real-time hardware-in-the-loop (HIL) studies similar to those that constitute the subject of this thesis. They use their HIL system to simulate their controls and FPGA hardware for the IEEE 13-bus test feeder, while supplementing their simulation with OpenDSS to simulate power flow in their distribution system. However, their OpenDSS simulation differs from the topic of this thesis in that it is not a microgrid; it is a standard distribution system with a substation and load buses, lacking generation and storage capabilities.

The authors of [8–10] use OpenDSS and a similar distribution framework, GridLAB-D, to model active distribution networks (ADNs) independent of other simulations. The simulations run in these studies are an attempt to use the various DERs to dynamically maintain power balance and optimize generator cost. Particularly, they emphasize control of storage resources and load shaping.

The great advantage of OpenDSS, evident in the current applications, is its flexibility to be applied effectively in different programming environments. Among the mentioned papers are OpenDSS implementations in MATLAB, Python, C/C++, Pascal, and even Microsoft Excel. The literature highlights the co-simulation capability of the simulation framework, one of the chief reasons it was chosen for this application.

CHAPTER 2

THE MICROGRID

This chapter focuses on the configuration and parameters of the microgrid to be simulated by OpenDSS. The network topology will be explored as generators, transformers, loads, and lines will be enumerated in detail. This microgrid is inspired by the TAC microgrid located in Champaign, Illinois. As the name suggests, this microgrid is mainly for research purposes, including testing of infrastructure resources, new distribution equipment, and development of smart grid technologies. Ameren Illinois and the University of Illinois at Urbana-Champaign can perform research jointly using these resources before wide-scale adoption [1]. In particular, this microgrid model will be used in research applications centered around distributed control of DERs to provide ancillary services to the bulk grid [11].

2.1 One-Line Representation

The microgrid to be modeled is illustrated by the one-line diagram shown in Figure 2.1. This model consists of 219 nodes on 8 buses. The diagram shows the high-level topology of the microgrid, including power generation, transformers, loads, transmission lines, and the tie-line connecting the microgrid to the bulk grid.

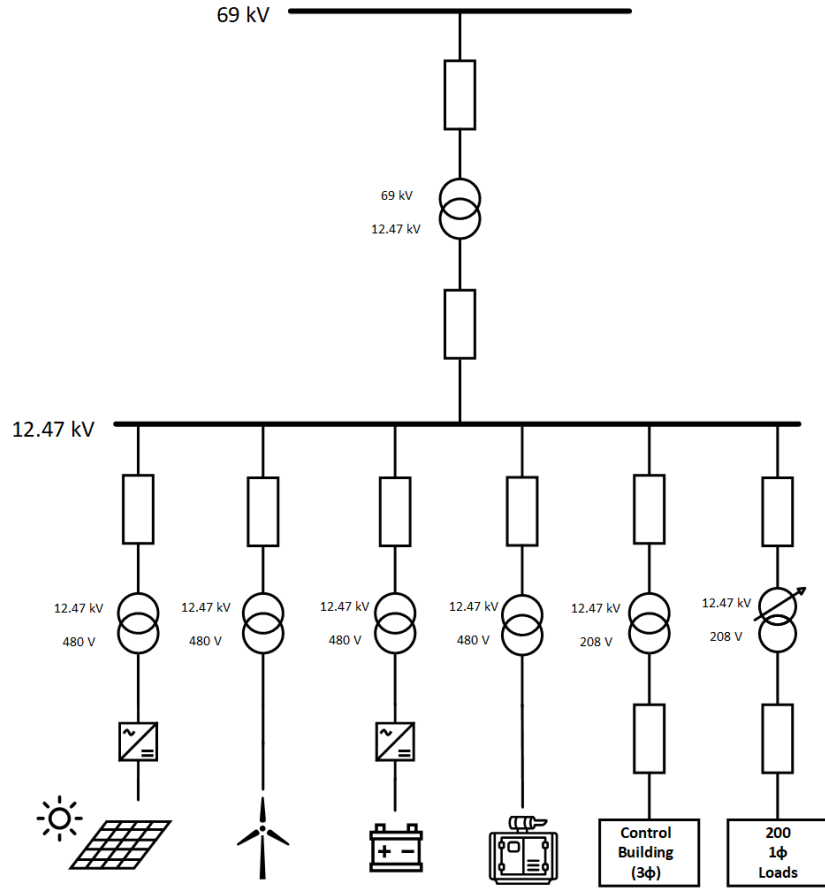


Figure 2.1: One-line diagram of the microgrid to be modeled

A top-level description of the network is as follows: an infinite 69 kV bus representing the bulk electrical grid is connected through a transmission line to a 69 to 12.47 kV transformer, located at the microgrid substation. This transformer is connected through transmission lines to four more transformers, 12.47 kV to 480 V, each connected to an independent DER: photovoltaic solar array (through an inverter), wind turbine, battery storage (through an inverter), and a natural gas driven synchronous generator. There are two load buses connected to the 12.47 kV substation bus: a single, 3-phase load representing the local substation controls and monitoring building, and a bus connecting to 200 single phase loads representing a large neighborhood. Both loads are connected to transformers stepping down the 12.47 kV to 208 V, with the addition of the neighborhood transformer having an on-load tap changer. This tap changer utilizes 33 taps (16 both above and below a center tap) at 0.625% per-tap for a total of nominal $\pm 10\%$, acting as a voltage regulator for the neighborhood.

2.2 Generators and Storage

The microgrid contains a total of four energy resources: solar array, wind turbine, natural gas generator, and lithium-ion battery storage. The two DC sources (solar and battery) are each connected to inverters, producing 480 V. The wind turbine and gas generators each produce power at 480 V as well. The generators and their respective parameters are tabulated in Table 2.1.

Table 2.1: DER Parameters

Element	Voltage [V]	Capacity [kW]	Note
GAS	480	1000	
SOLAR	480	125	Inverter
WIND	480	100	
BATT	480	250	Inverter, rated 500 kWh

2.3 Transformers

There are a total of 7 transformers in the system. Their parameters are outlined in Table 2.2 (note that the superscripts P and S refer to “primary” and “secondary”, respectively). As mentioned previously, the transformer responsible for the neighborhood connection is a tap-changing-under-load (TCUL) transformer, acting as a voltage regulator for the neighborhood bus. For the sake of this model, the tap changer was set to monitor the voltage on phase C of the load bus (chosen arbitrarily). Because load magnitudes are reasonably balanced in the testing scenarios presented, this single-phase monitoring is sufficient to control the voltage.

Table 2.2: Transformer Parameters

Element	Voltage ^P [kV]	Voltage ^S [kV]	Bus ^P	Bus ^S
T.SUB	69	12.47	B_GRID	B.SUB
T.SOLAR	12.47	0.480	B.SUB	B.SOLAR
T.WIND	12.47	0.480	B.SUB	B.WIND
T.GAS	12.47	0.480	B.SUB	B.GAS
T.BATT	12.47	0.480	B.SUB	B.BATT
T.CONTR	12.47	0.208	B.SUB	B.CONTR
T.NEIGHB	12.47	0.208	B.SUB	B.NEIGHB

CHAPTER 3

MODELING IN OPENDSS

3.1 Buses

The OpenDSS framework requires the explicit enumeration of buses in the system. Each element must be connected to one or more buses, depending on the element type. A complete list of buses is shown in Table 3.1.

Table 3.1: Buses in Network

Bus	Voltage [V]
B_GRID	69k
B_SUB	12.47k
B_SOLAR	480
B_WIND	480
B_BATT	480
B_GAS	480
B_CONTR	208
B_NEIGHB	208

These buses form the framework of the model. Every element within the network is connected to one or more buses either directly or through a distribution line.

3.2 Lines

There are 10 transmission lines in the network. They are modeled based upon per-unit-length impedance taken from the EPRI Test Circuit 5 [2]. In the network, there exists a transmission line between any two connected nodes,

with two exceptions. The distance between the energy resources and their corresponding transformers was deemed negligible, and thus line impedances between these nodes are neglected. Additionally, the 200 single-phase neighborhood loads are not all individually connected via separate lines. The transmission line traveling from the substation to the neighborhood is modeled, whereafter all the loads are connected directly to its termination, with no final “line-to-home” impedance. Line connections and parameters including per-unit-length impedance at 60 Hz are detailed in Table 3.2.

Table 3.2: Distribution Line Parameters

Line	Conn 1	Conn 2	L [km]	R [$\frac{\Omega}{\text{km}}$]	X [$\frac{\Omega}{\text{km}}$]	C [$\frac{\text{nF}}{\text{km}}$]
L1	B_GRID	T_SUB_P	1.0	0.0656	0.193	3.165
L2	T_SUB_S	B_SUB	0.2	0.0656	0.193	3.165
L3	B_SUB	T_SOLAR_S	0.3	0.0656	0.193	3.165
L4	B_SUB	T_WIND_S	0.1	0.0656	0.193	3.165
L5	B_SUB	T_BATT_S	0.1	0.0656	0.193	3.165
L6	B_SUB	T_GAS_S	0.1	0.0656	0.193	3.165
L7	B_SUB	T_CONTR_P	0.1	0.0656	0.193	3.165
L8	T_CONTR_S	B_CONT	0.01	0.0656	0.193	3.165
L9	B_SUB	T_NEIGHB_P	2.0	0.0656	0.193	3.165
L10	T_NEIGHB_S	B_NEIGHB	1.0	0.0656	0.193	3.165

3.3 Initial Simplified Model

The model was initially created in a highly reduced fashion. All generator buses were treated simply as PV buses (real power and voltage given), and load buses were treated as PQ buses (complex power given). Transformers were ideal, shifting voltage levels with no losses. From here, the network was connected using the parameters given in Tables 2.1, 2.2, 3.1, and 3.2. OpenDSS was used as a power flow calculator for the network, solving the

standard power flow equations [12].

$$P_k = \sum_{j=1}^N |V_k||V_j| (G_{kj} \cos(\theta_k - \theta_j) + B_{kj} \sin(\theta_k - \theta_j)) \quad (3.1)$$

$$Q_k = \sum_{j=1}^N |V_k||V_j| (G_{kj} \sin(\theta_k - \theta_j) - B_{kj} \cos(\theta_k - \theta_j)) \quad (3.2)$$

Here P_k and Q_k are the net real and reactive powers injected at bus k , and G_{kj} and B_{kj} are the real and imaginary components of the kj entry in the bus admittance matrix. OpenDSS calculates the admittance matrix and solves the equations.

Using this ideal model, a preliminary no-load simulation was run to ensure the proper setup of the model. In this scenario, the DERs were assigned arbitrary outputs, in keeping with the PV nature of the model. These outputs were varied 5 times, with OpenDSS simulating the network behavior after each variation. Figures 3.1 and 3.2 show the per-phase real generation and tie-line voltage for this simulation.

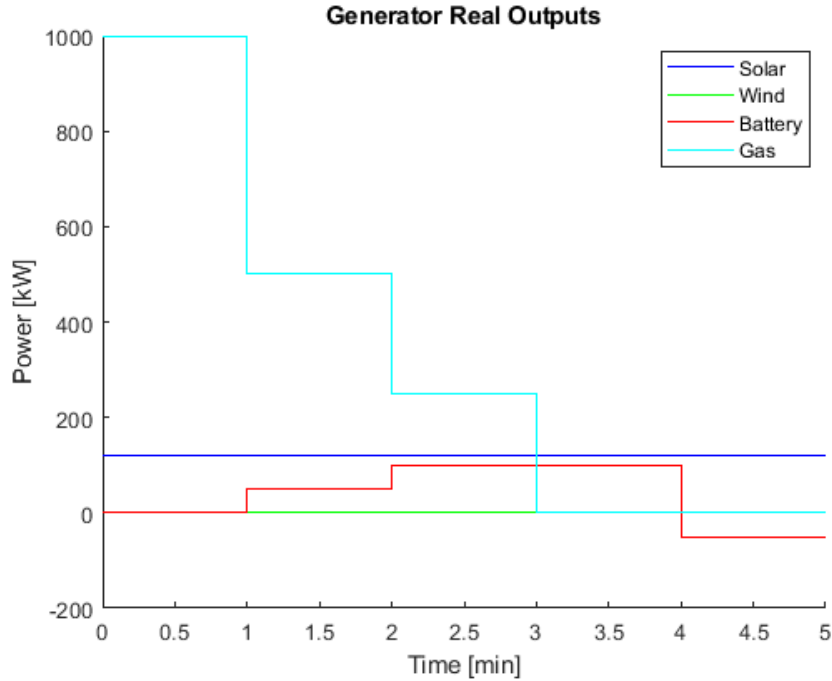


Figure 3.1: Real power generated in preliminary test

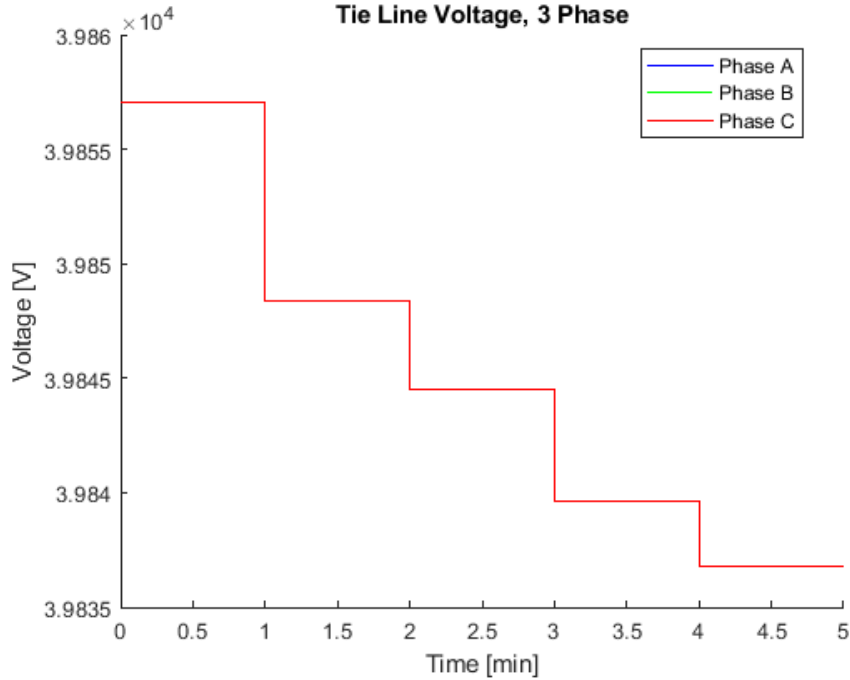


Figure 3.2: Tie line voltage in preliminary test

This initial no-load simulation shows that the model does seem to be working as intended, with the generators causing voltage effects on the tie-line (the expected increase in generation causing an increase in voltage). However, the changes to the system are instantaneous and not reflective of real-world behavior. To remedy this, the model was refined with the goal of successfully simulating an “normal” day in central Illinois.

3.4 Refined Model

3.4.1 Inverter-Based Source Models

Rather than simply arbitrarily assigning power outputs to the solar and battery units, a more realistic representation is desired.

The active power output of the solar array is a function of the solar irradiance E_e , ambient temperature T , and a power rating. This power rating, P_{mpp} , is equal to the real power produced at the maximum power point for a given temperature (this case 25°C) and irradiance of $1.0 \frac{\text{kW}}{\text{m}^2}$ [13]. The inverter behavior is abstracted out by applying an efficiency factor (η_{inv}) to

the array output [14]. Therefore the output power of the solar array given certain environmental parameters can be calculated.

$$P_{array} = P_{mpp} \cdot E_e \cdot K_t \cdot \eta_{inv} \quad (3.3)$$

The temperature factor K_t is provided by the manufacturer of the panel. For this simulation, the factor from the Yingli 60-series solar modules in use at the TAC was used [15].

$$K_t = 1 - 0.17 \cdot (T - 25) \quad (3.4)$$

The efficiency factor for the inverters used for both the solar array and the battery unit was taken from the California Energy Commission (CEC) experimental efficiency database matching the voltage and rated power of this solar array [14]. The efficiency curve [14] is shown in Figure 3.3.

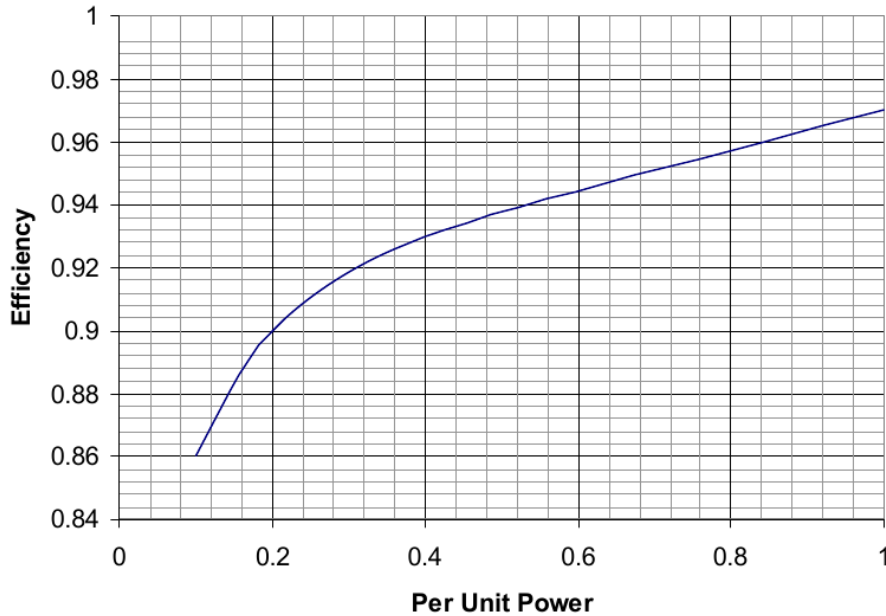


Figure 3.3: Inverter efficiency curve

As shown, the AC power output of the solar array in the model will have a maximum of $\approx 97\%$ of its maximum output before the inverter at a given temperature, with a minimum of $\approx 86\%$ at lower power levels, such as during overcast periods, or the sunrise/sunset periods. This inverter efficiency curve is also used for the battery storage unit for simplicity.

3.4.2 Historical Location Data

To perform as accurate a daily simulation as possible, it is crucial to use realistic data in setting power output levels for the sources in the system. As such, historical environmental data from Decatur, Illinois, (approximately 50 miles southwest of Champaign), is used to calculate the outputs of the solar and wind energy sources. This data includes temperature (T), solar irradiance (E_e), and wind speed (v_{wind}) for July 21, 2017 [16–18]. It was assumed for this simulation that the wind turbine is always optimally aligned with the wind direction. The temperature and solar irradiance data for the chosen date are shown in Figures 3.4 and 3.5.

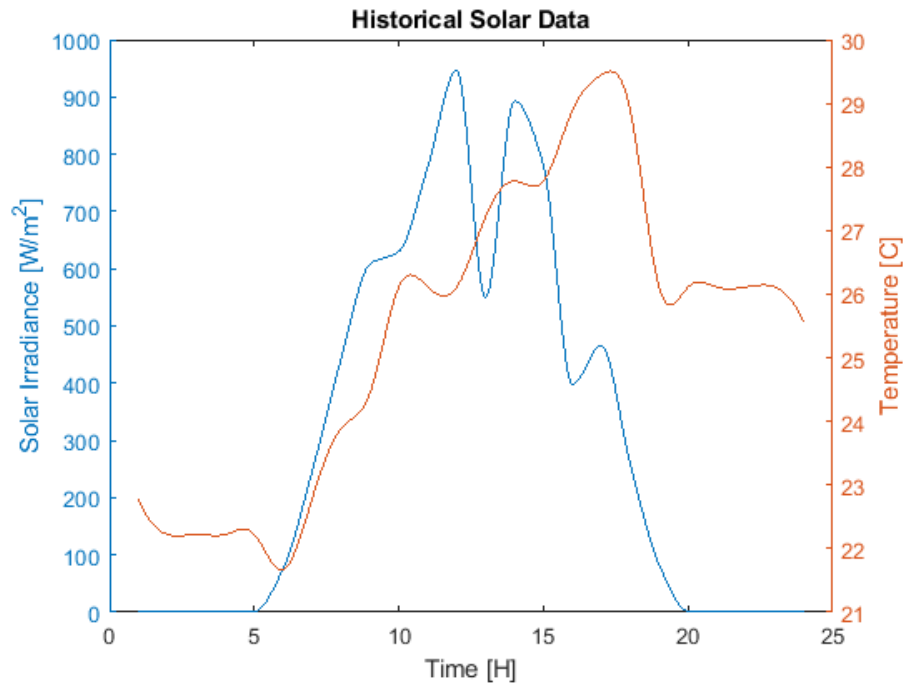


Figure 3.4: Historical solar data, Decatur, IL, 07/21/2017

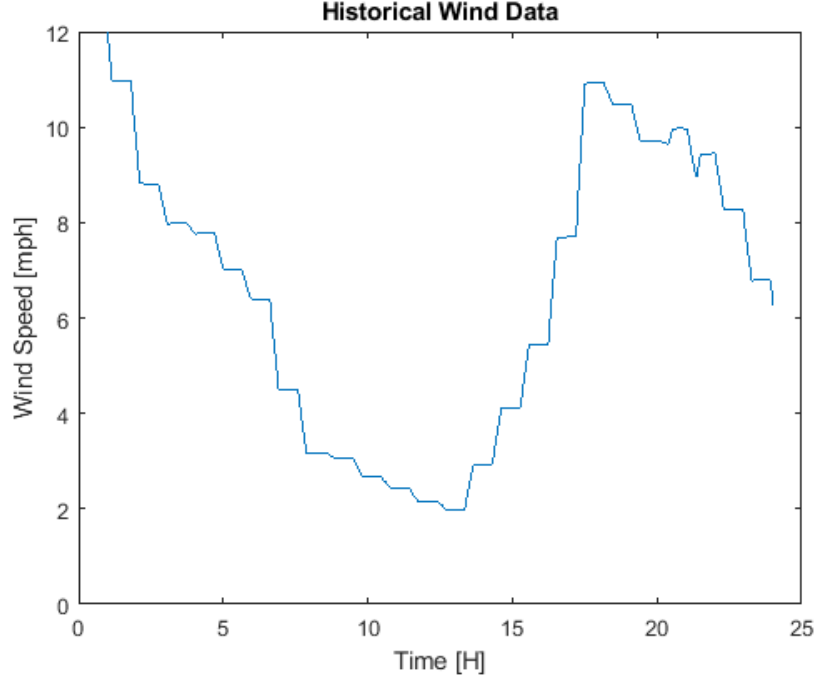


Figure 3.5: Historical wind data, Decatur, IL, 07/21/2017

The solar data was fed into the model based upon Equations 3.3 and 3.4. The wind data was used to calculate the power output of the wind turbine using equation 3.5.

$$P_{out} = \frac{1}{2} \rho A v_{wind}^3 C_p \quad (3.5)$$

Here ρ is the density of the air at the altitude and mean temperature of Decatur ($\rho \approx 1.17 \frac{\text{kg}}{\text{m}^3}$), A is the swept area of the blades ($A \approx \pi \cdot 10^2 = 314.2 \text{ m}^2$ given 10 m blade length). The power coefficient C_p is set to the Betz limit of 0.59, assuming maximum efficiency of the wind turbine [19]. These power outputs were calculated for each data point and then fed to the model.

3.4.3 Load Models

To accurately simulate a day's operation, it is necessary to develop loadshapes to describe the power draw of the neighborhood loads. In this scenario, the creation of 200 independent load shapes is infeasible. To solve this problem, 3 independent loadshapes were developed, with each household load taking

on a linear combination of each shape. Using the method described in [20], these loadshapes were determined based on the assumption that most homes contain certain common appliances (refrigerator/freezer, electric oven/stove, microwave oven, heating/cooling, television, lighting), while a smaller number of homes contain more “luxury” appliances (clothes washer/dryer, dishwasher, personal computer). Note that due to the fact that the day chosen to be simulated is July 21st, air-conditioning was assumed to be in heavy use for most of the day. The generated load shapes are plotted in Figure 3.6.

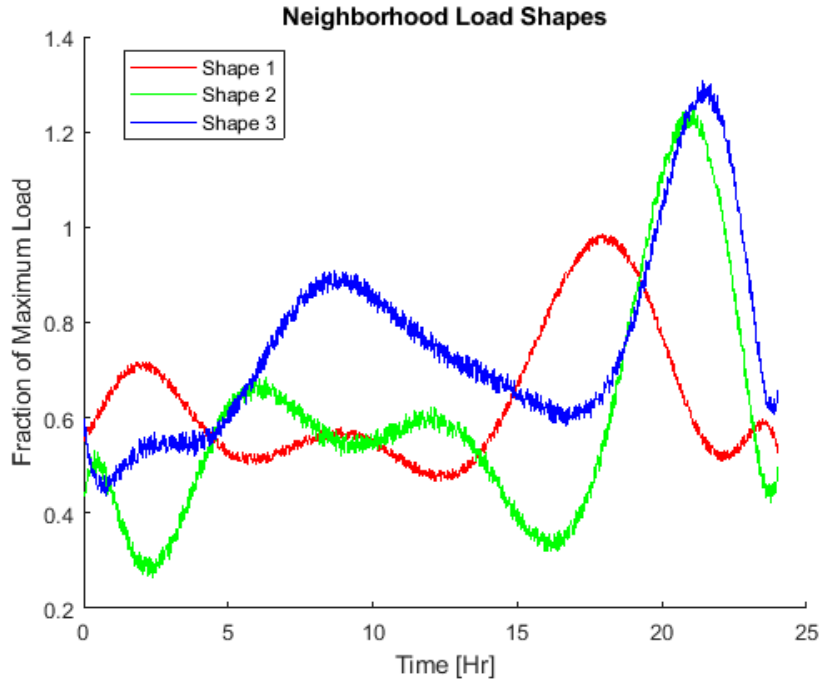


Figure 3.6: Generated load shapes

These three shapes form the basis of the neighborhood loads. In the MATLAB driver, each of the 200 residential loads is formed by a linear combination of these shapes.

$$\text{load}_n = k_{n1}S_1 + k_{n2}S_2 + k_{n3}S_3 \quad (3.6)$$

Here S_1 , S_2 , and S_3 are the load shapes, and k_{n1} , k_{n2} , and k_{n3} are randomly chosen constants between 100 and 700, such that the power draw per home lies between a maximum of 2.1 kW and minimum of 300 W [20]. These loads are then evenly distributed across the three phases of the load bus (66 phase A, 66 phase B, and 67 phase C), in an attempt to make the system

quasi-balanced. The total three-phase load of the neighborhood is shown in Figure 3.7.

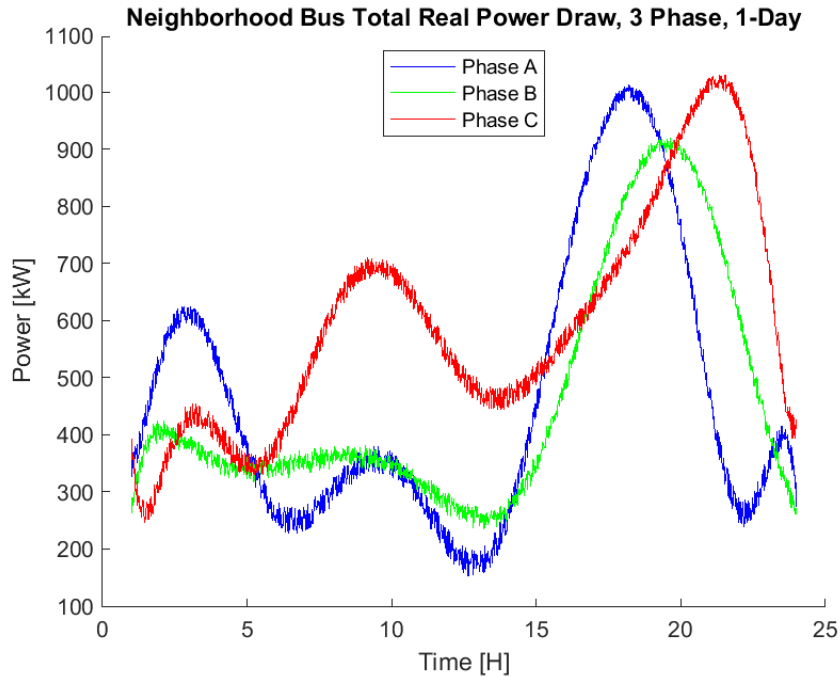


Figure 3.7: Combined neighborhood load, per phase

Because the function of the control building is constant monitoring and control, the load is assumed for the purposes of this simulation to be constant. A value of 65 kW was chosen. It must be lit and climate controlled for the entire duration of the day, along with sensory and control equipment being run constantly, making this a fair assumption.

3.4.4 Full-Day Simulation

The simulation was run for the full day model, using the real-world data from July 21, 2017. For simplicity, it was assumed that the gas generator was running at 90% capacity for the duration of the day, and that the microgrid was operating in grid-connected mode; that is, power was able to freely pass either direction along the tie line. The results of the simulation are shown in Figures 3.8 through 3.11.

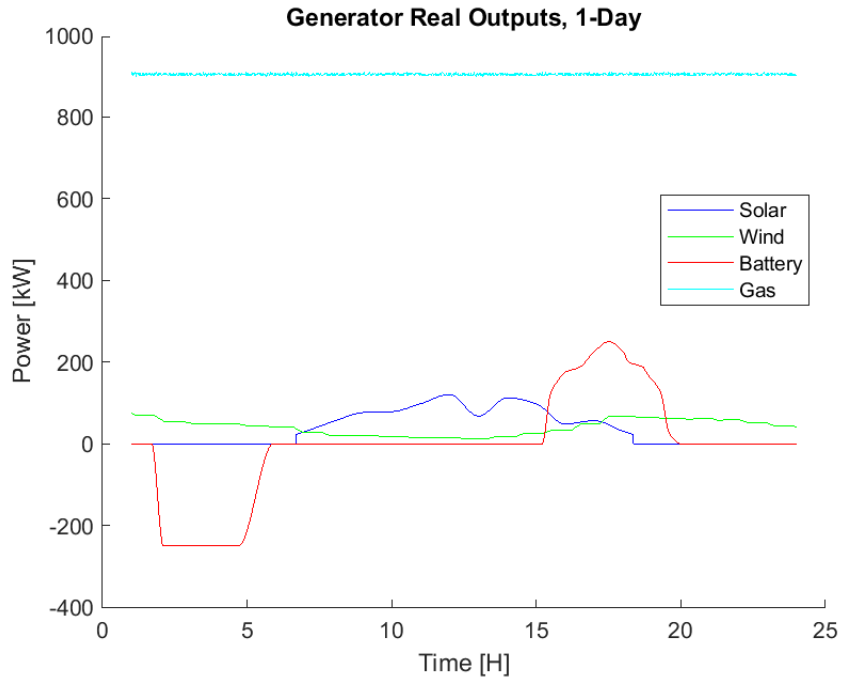


Figure 3.8: Simulated generation, full day

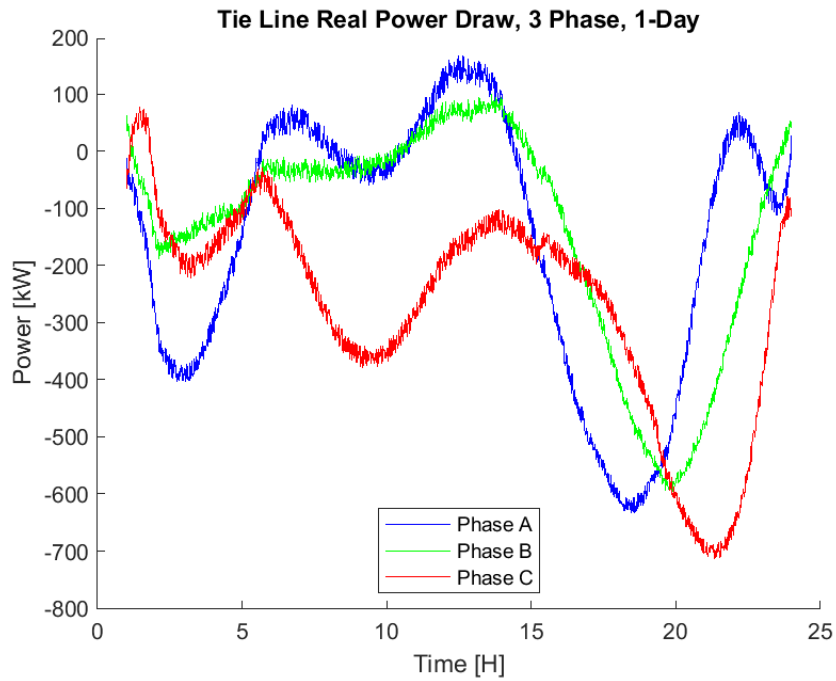


Figure 3.9: Simulated power exchanged on tie-line, full day

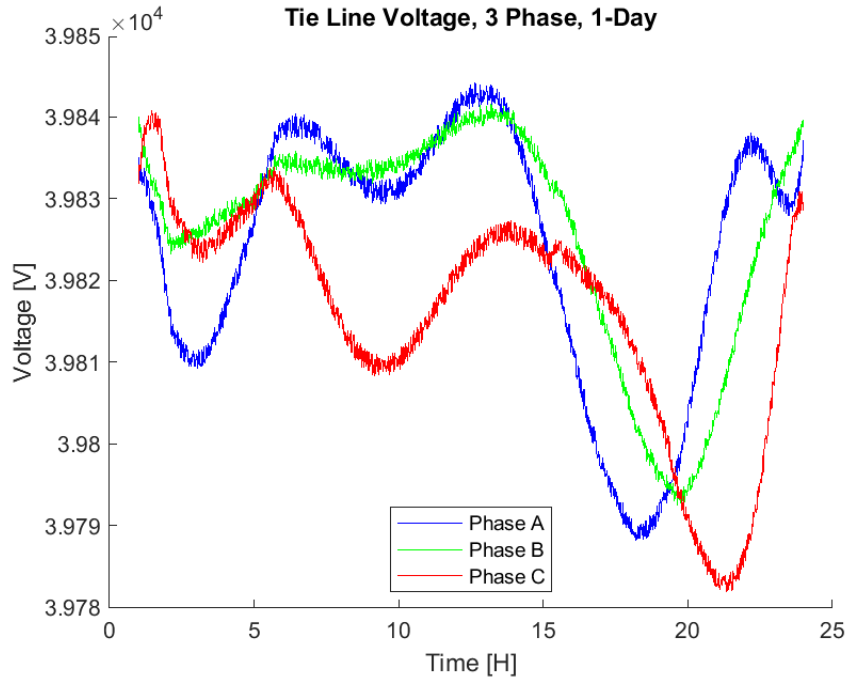


Figure 3.10: Simulated voltage on tie-line, full day

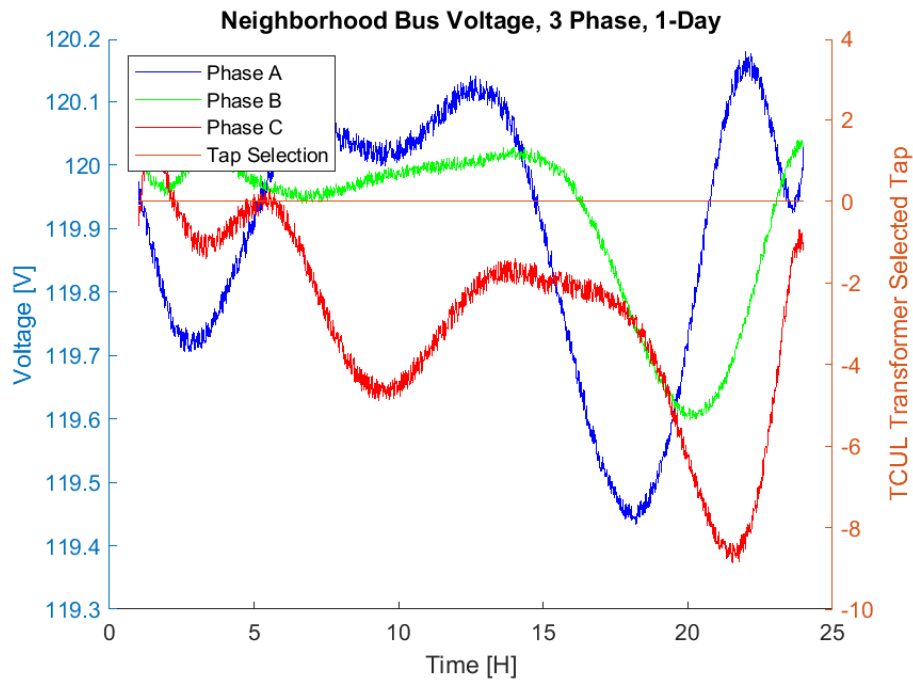


Figure 3.11: Simulated voltage on neighborhood bus, full day

Figure 3.8 shows the generation of all modeled sources. The renewable sources generally follow the previously discussed curves, with the addition

of the sharp “turn-on” step of the solar array, taking the minimum power capability of the attached inverter [21]. The battery storage in this case is used in an attempt to ease the burden on the bulk grid during the heavy power-consuming portion of the day. It charges during the low-load period overnight, and discharges during peak hours. Figure 3.9 shows the power exchanged with the bulk grid through the tie-line. Negative values indicate power flowing into the microgrid, and positive values indicate power flowing out of the microgrid. The simulation indicates that for this particular day and with the gas generator running at 90% capacity, the microgrid both draws power from and supplies power to the grid depending mostly upon the demand of the neighborhood. The voltage plots in Figures 3.10 and 3.11 show that across the day, the tie-line voltage varied by approximately 0.15% and the neighborhood voltage varied by approximately 0.6%. The voltage swings on the neighborhood bus were not enough to trigger the tap changer ($\pm 0.625\%$), so it remained at the center tap for the duration of the day. A subsequent simulation was run with artificially inflated load values to specifically verify that the tap changer behaves as desired. The results of that simulation are shown in Figures 3.12 and 3.13.

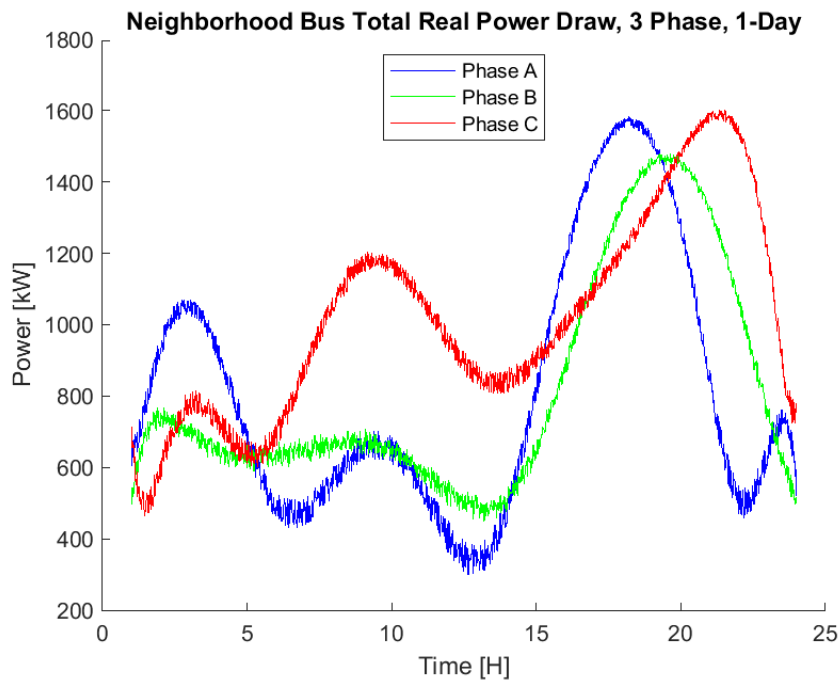


Figure 3.12: Artificially inflated loads

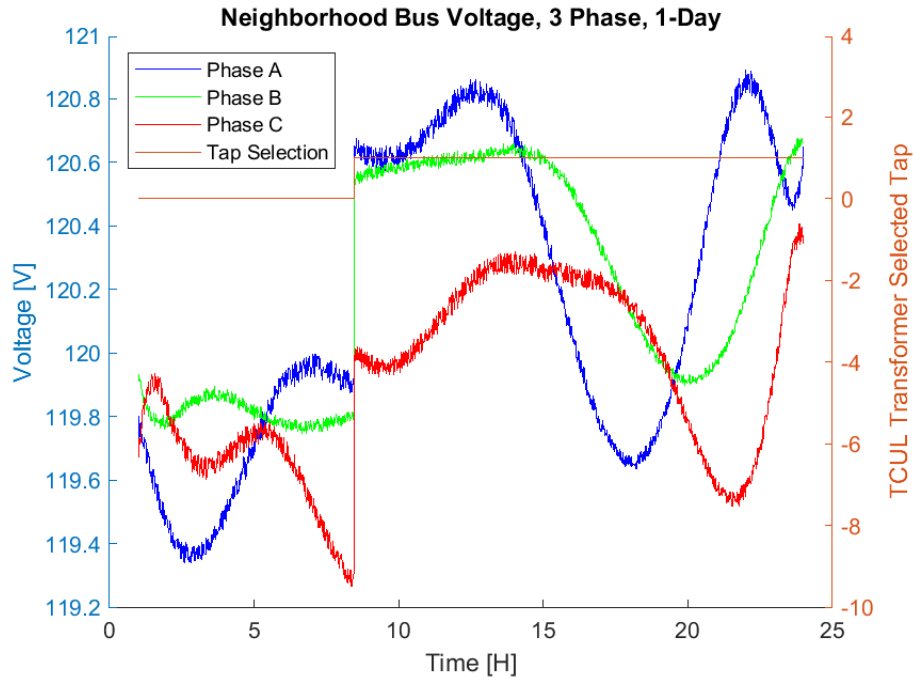


Figure 3.13: Neighborhood voltage response to artificially inflated loads

As the neighborhood load increases, the voltage starts to drop. When it has dropped by the requisite $0.625\% = 0.75$ V, the tap changer (monitoring Phase C) switches to tap 1 to boost voltage back to desired levels, as expected.

3.5 Auxiliary Implementation of Dynamics

Though OpenDSS simulates the network discretely, dynamics can be added in an auxiliary fashion by the driver program [2,3]. Rather than issuing the simulator step commands as in previous simulations, the operator can define the desired dynamic behavior within MATLAB. For example, dynamics were added to the gas generator by calculating its dynamic response to a step command in output power. This response was calculated, and then fed to the simulator, allowing the network to be solved for this dynamic behavior.

3.5.1 Generator Model

The synchronous generator was modeled as described in [12] in $dq0$ rotor-flux reference frame. This model is outlined in the following equations.

$$\lambda_d = L_d i_d + L_{af} i_f \quad (3.7)$$

$$\lambda_q = L_q i_q \quad (3.8)$$

$$\lambda_f = \frac{3}{2} L_{af} i_d + L_{ff} i_f \quad (3.9)$$

$$\lambda_0 = L_0 i_0 \quad (3.10)$$

$$v_d = R_a i_d + \frac{d\lambda_d}{dt} - \omega_m \lambda_q \quad (3.11)$$

$$v_q = R_a i_q + \frac{d\lambda_q}{dt} + \omega_m \lambda_d \quad (3.12)$$

$$v_f = R_f i_f + \frac{d\lambda_f}{dt} \quad (3.13)$$

$$v_0 = R_a i_0 + \frac{d\lambda_0}{dt} \quad (3.14)$$

$$T_{mech} = \frac{3}{2} \left(\frac{p}{2} \right) (\lambda_d i_q - \lambda_q i_d) \quad (3.15)$$

Using this model, machine dynamics can be calculated. Of particular interest is the machine response to step commands in power output. Using MATLAB, the dynamic response to such a command is able to be quickly calculated. This response, rather than the step command itself, is then passed to the OpenDSS network for simulation.

A no-load simulation was run to verify the operation of the simulator in response to such dynamical inputs. All additional energy sources were also set to 0 to capture only the system response to the generator. The test was run for a duration of 2.5 seconds, with a step command issued at $t = 1.1$ s to increase output power of the generator from 460 to 700 kW. The simulated generator output and tie-line exchange are plotted in Figures 3.14 and 3.15.

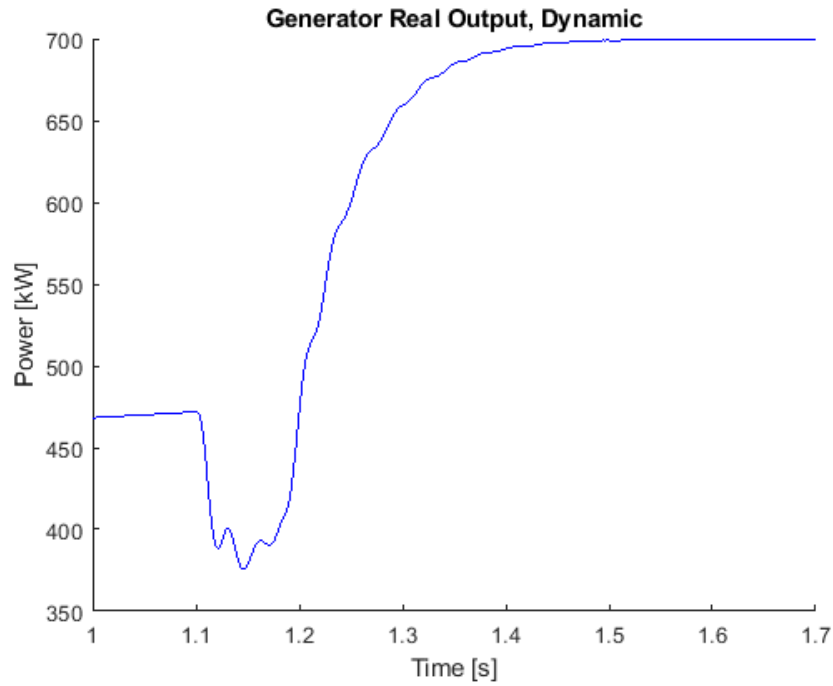


Figure 3.14: Generator dynamic test

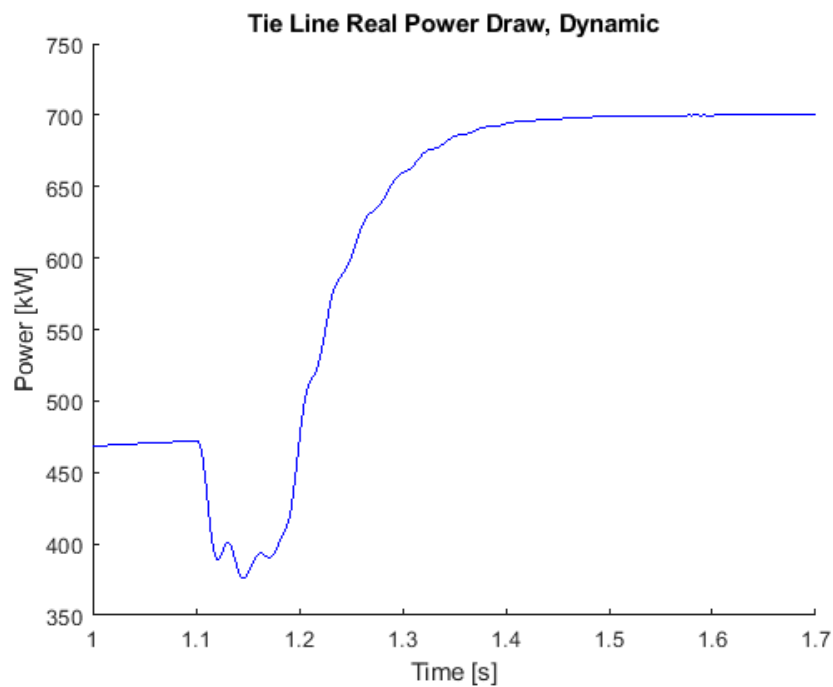


Figure 3.15: Dynamic tie-line exchange

The simulation is able to take this dynamic input and show that its effects are translated through the network. By implementing a dynamic model

in MATLAB, some dynamics are able to be introduced into the OpenDSS simulation.

CHAPTER 4

AN APPLICATION IN DISTRIBUTED CONTROL STUDIES

As noted before, the goal of this model is to be able to insert it into other simulations on an as-needed basis, rather than creating a bespoke model for every single research application. This chapter presents the use of an OpenDSS microgrid model in co-simulation with the C-HIL testbed developed at UIUC [11]. While the model used in this application is not the same as the one used in previous chapters due to the milestone requirements of the project, the developed simulation interface and procedure are exactly the same; the previously described microgrid could be used to seamlessly replace the one used here. The microgrid model used in this application was developed in cooperation with researchers at the University of California, San Diego [11].

4.1 Co-simulation Goals

The goal of the project was to test the real-world viability of distributed control techniques developed by the ARPA-E NODES group at UIUC. The purpose of this control is to allow an ISO to directly control the power output of a microgrid to provide ancillary services to the grid at large. The chief requirements for this milestone are that the system meet a maximum initial response time of 5 seconds and that the reserve magnitude variability of the output be less than $\pm 5\%$. In this particular case, the goal is frequency regulation. As mentioned previously, this is accomplished in a distributed manner, with controllers located at each controllable node communicating together to calculate the desired power output of each node necessary to reach the request of the Independent System Operator (ISO) [11].

4.2 Microgrid Model

The milestone requires the use of the microgrid in use on-campus at UCSD. This model is a radial, balanced network with 3867 nodes and 1289 buses. Generation is handled by a combination of photovoltaic, gas, and steam turbines. Loads are composed of buildings and electric vehicle charging stations. Because the present capability of the C-HIL testbed is 100 controllable nodes, this model had to be reduced using the distribution feeder reduction algorithm described in [22].

The reduced model used in this simulation contains 13 generators (10 photovoltaic) and 107 loads for a total of 120 nodes.

4.3 Simulation

Because the UIUC C-HIL testbed is only capable of simulating 100 controllable nodes at the present time, 20 of the microgrid nodes were held constant. The nodes chosen were 20 load nodes. For the duration of the simulation, these nodes consumed a constant amount of complex power.

An additional consideration had to be taken into account, as loads are typically not controllable and there are not 100 generators in the system. After taking the 13 generators into account, the remaining 87 controllable nodes had to be loads. To accomplish this in simulation, these nodes were treated as generators creating “negative” power.

4.3.1 C-HIL Testbed Interface

The chosen environment to interface the testbed and the OpenDSS simulation was MATLAB. This was chosen due to its robust mathematical capabilities, ease of communication, and extensive OpenDSS driver documentation.

The simulation procedure is outlined as follows:

1. ISO sends signal to distributed controllers containing desired power output of microgrid
2. Controllers communicate and arrive at necessary node setpoints via ratio consensus algorithm [11]

3. Controllers update generator outputs with new setpoints
4. Generators adjust power output in response to updated setpoints
5. Microgrid power flow is simulated (OpenDSS), tie-line power exchange is calculated and compared to ISO's desired value
6. Controllers hold setpoints until new ISO command is received

During simulation, the ISO sends its signal through MATLAB via the Modbus protocol to the controllers. After reaching consensus on the desired setpoints, the controllers then independently update their generators. In a real-world scenario, these controllers would be attached to their generators. In simulation, they each independently (to preserve the integrity of the distributed framework) communicate values to a separate MATLAB instance via Modbus again. This MATLAB instance is the driver for the OpenDSS simulation. After updating each node with its new output value, the OpenDSS simulation is then run, recording the tie-line power exchange. This architecture is illustrated in Figure 4.1, developed by the NODES group [11].

4.3.2 First Experimental Scenario

Three simulation scenarios were performed to test the efficacy and accuracy of the simulation. They were all variations in the input ISO signal.

The first input signal tested was a “stepped ramp” signal, simply to test the microgrid response. This consisted of stepping the regulation signal from 0.2 to 0.7 over a period of approximately 2 minutes. This regulation signal corresponds to a command requesting an increase in output 0.2 to 0.7 times the difference between the initial power output and the total capacity. The results of this first experiment are shown in Figure 4.2.

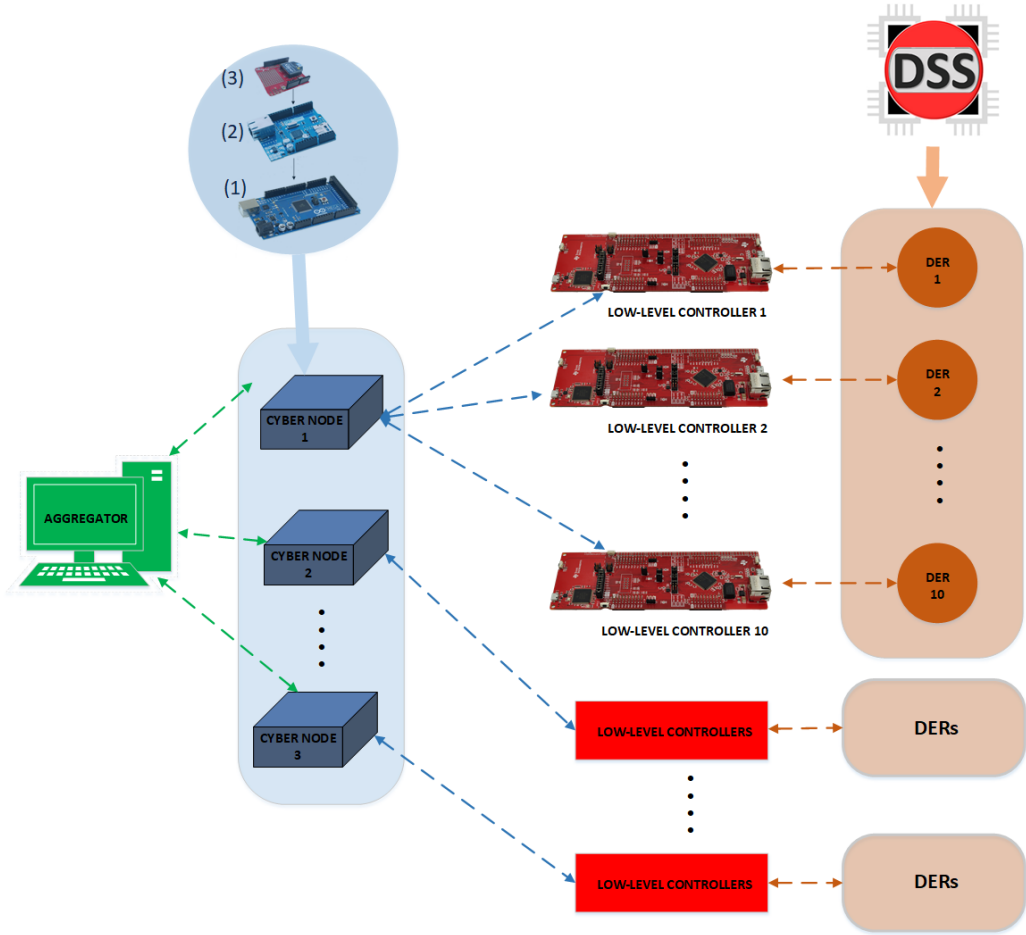
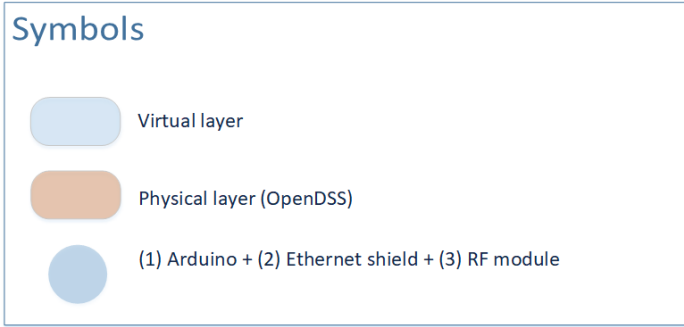


Figure 4.1: System architecture for C-HIL co-simulation

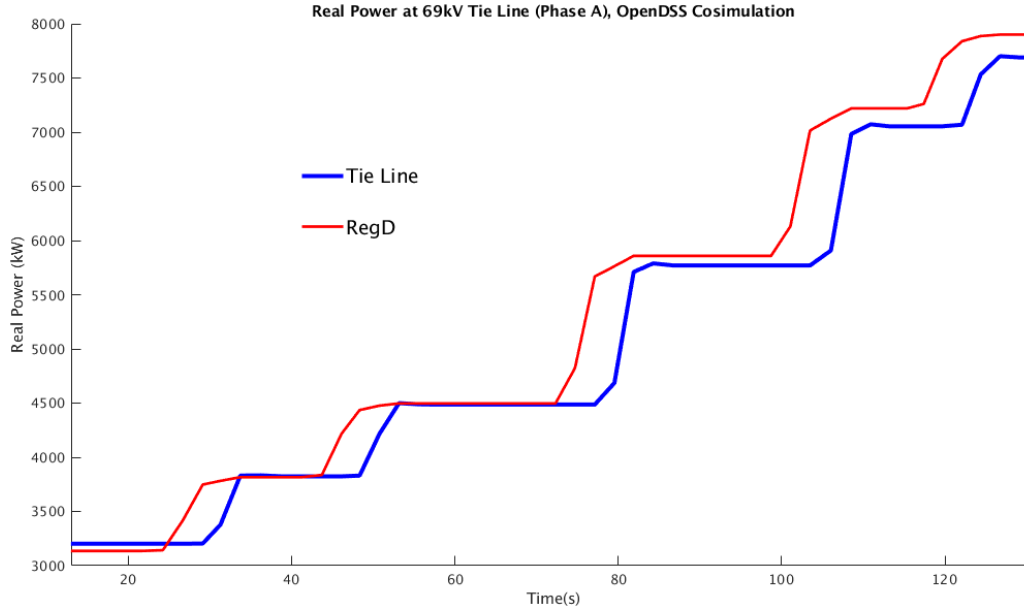


Figure 4.2: Simulation results for “stepped ramp” input signal

The results show the microgrid simulation output generally following the input signal. There is a delay between the signal send time and the response, which corresponds to the communication delay between the components of the system, as well as the time required by the distributed controllers to come to consensus (between 4.2 to 4.7 seconds, depending on the connection graph of the controllers). This, however, meets the requirement of a 5-second initial response time. The simulation shows that the power generated by the microgrid is not exactly equal to the requested value. This error is introduced by two sources in the model. The first is the transmission loss combined with the constant loads present in the model. These loads are consuming some set amount of power for the duration of the simulation, and are not taken into account by the control scheme. The second is the transmission loss. The power measured at the tie line is equal to the generated power (commanded by the ISO), less the line losses from all nodes to the interconnect. These errors could both be corrected in future simulations by factoring them into how the updated power setpoints are calculated.

4.3.3 Second Experimental Scenario

The second input signal tested was the first 5 minutes of the PJM RegD wave. The PJM interconnect is a regional transmission organization (RTO) that operates in 13 states in the eastern United States. As part of their service, they provide a 40-minute regulation self-test signal to aid in development of technologies to provide ancillary support to the grid. The results of this simulation of the first 5 minutes of the signal are shown in Figure 4.3.

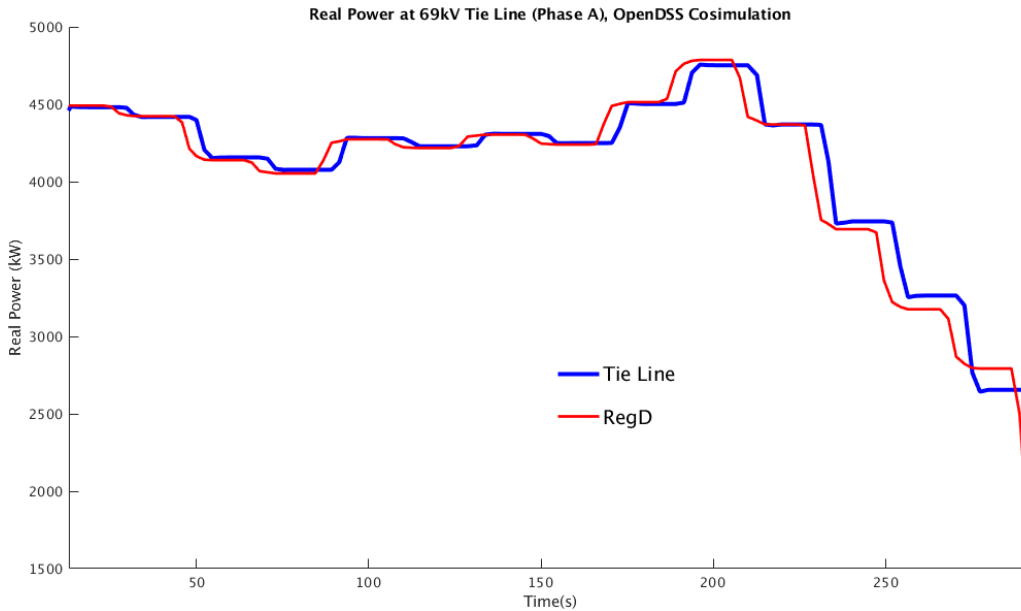


Figure 4.3: Simulation results for first 5 minutes of PJM RegD signal

The goal of this scenario was to test the model’s response to a steeply decreasing signal. Again, the results show that the controllers are able to accurately control the tie-line power injection from the microgrid, with the same error sources appearing as in the first test, and with some calculation/communication delay.

4.3.4 Third Experimental Scenario

The third scenario tested was the second 5 minutes of the same PJM RegD wave (Figure 4.4). This simulation was conducted to test the system’s response to a steeper increasing signal. Again, the same errors and delays are present in the results, with the possibility of being compensated for in future

trials. The system is able to respond adequately to the input commands, providing the requested power within the required $\pm 5\%$ tolerance for reserve magnitude variability, even when not compensating for system losses and unmodeled loads.

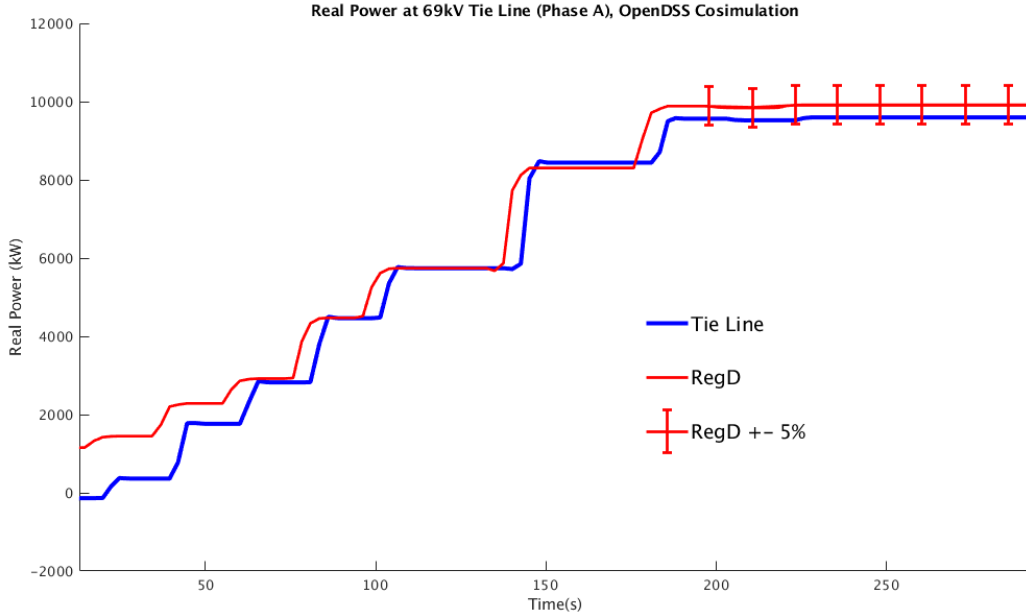


Figure 4.4: Simulation results for second 5 minutes of PJM RegD signal

To ensure that the requirements of the test are being met, the signal is held constant at the end of the test, showing that the microgrid is able to hold the $\pm 5\%$ magnitude variability.

These simulations confirm that the distributed control is being performed to meet the time and accuracy requirements, and able to accurately communicate with the OpenDSS model of the real-world network. The simulation results of the model show that the system is responding as requested, and that, even without losses taken into account, the required metrics are still being met.

CHAPTER 5

CONCLUSIONS AND FUTURE WORK

This thesis describes a model in the OpenDSS framework of a generic microgrid based upon Ameren’s TAC microgrid located in Champaign, Illinois. The creation of this model is motivated by the need to evaluate the performance of distributed control algorithms, currently under development by the NODES group in the Power and Energy Systems area at UIUC. Because the full dynamic simulation of such a microgrid would be computationally intensive, a method for simulating microgrid response to control inputs without the full dynamic performance is required. This OpenDSS model allows for the simulation of the microgrid with only the dynamics that the designer deems appropriate incorporated, reducing computation time and speeding up the simulation process.

The microgrid consists of four energy resources (solar array, wind turbine, natural gas generator, and battery storage), 201 loads, including 200 realistically modeled household loads distributed equally among the three electrical phases, and a single load representing the control center for the microgrid. These sources and loads are each connected through a series of transformers to the microgrid substation, where another transformer links the microgrid to the bulk grid through a single tie-line. The key conclusions and products of this thesis are as follows:

- A dynamics-free model of a microgrid based upon Ameren’s TAC microgrid is available for use, with the option of adding dynamics on a node-by-node basis in the driver program.
- While specifically designed with the Typhoon C-HIL laboratory in mind, the model may be co-simulated with any necessary application, through interfaces written in C, Python, and MATLAB, among others.
- Co-simulations between OpenDSS and the C-HIL distributed control architecture were successful, demonstrating the efficacy of both the

model and the controller architecture.

This model may be useful in many research applications, and future work may include the following:

- Further implementation of dynamics into the driver code. Presently, only generator dynamics are included, and only on an as-needed basis. However, due to the nature of the model, further dynamic models may be incorporated, particularly in transformer behavior. Simulation could be further improved by adding control schemes around the applied dynamical models.
- More realistic battery behavior, including optimal charge/discharge periods and different deployment strategies.
- Simulations of this microgrid in islanded mode. Though this model is primarily built for co-simulation, with grid service-providing ends, this model could be used independently, with particular interest in its capability of simulating the microgrid in islanded mode, something not explored in this thesis.
- Development of a driver program using Python in keeping with the open-source nature of the simulation.

REFERENCES

- [1] M. Hagge and O. Doyle, “Ameren Illinois TAC microgrid.” Presented at PECE 2018 Conference, Champaign, Illinois, February 23, 2018.
- [2] D. Montenegro and R. C. Dugan, *Reference Guide, The Open Distribution System Simulator (OpenDSS)*. EPRI, March 2018.
- [3] A. Arguello, W. L. Cunha, T. R. Ricciardi, R. Torquato, and W. Freitas, “Dynamic modeling in OpenDSS: An implementation sequence for object Pascal,” *2018 IEEE Power & Energy Society General Meeting (PESGM)*, 2018.
- [4] A. Hariri, A. Newaz, and M. O. Faruque, “Open-source Python-OpenDSS interface for hybrid simulation of PV impact studies,” *IET Generation, Transmission & Distribution*, vol. 11, no. 12, p. 3125–3133, 2017.
- [5] J. A. Ahamioje and H. Krishnaswami, “Interconnection study of distributed PV systems by interfacing Matlab with OpenDSS and GIS,” *2017 IEEE 44th Photovoltaic Specialist Conference (PVSC)*, 2017.
- [6] D. Montenegro, M. Hernandez, and G. A. Ramos, “Real time OpenDSS framework for distribution systems simulation and analysis,” *2012 Sixth IEEE/PES Transmission and Distribution: Latin America Conference and Exposition (T&D-LA)*, 2012.
- [7] L. C. Ribeiro, J. P. O. S. Minami, B. D. Bonatto, P. F. Ribeiro, and A. C. Z. D. Souza, “Voltage control simulations in distribution systems with high penetration of PVs using the OpenDSS,” *2018 Simposio Brasileiro de Sistemas Eletricos (SBSE)*, 2018.
- [8] W. Guo, J. Lin, Y. Song, and X. Chen, “A simulation platform of active distribution network based on co-simulation of GridLAB-D and Matlab,” *2014 International Conference on Power System Technology*, 2014.
- [9] D. P. Chassin, K. Schneider, and C. Gerkenmeyer, “GridLAB-D: An open-source power systems modeling and simulation environment,” *2008 IEEE/PES Transmission and Distribution Conference and Exposition*, 2008.

- [10] J. Ma, F. Yang, Z. Li, and S. J. Qin, “A renewable energy integration application in a microgrid based on model predictive control,” *2012 IEEE Power and Energy Society General Meeting*, 2012.
- [11] C. Sain, S. Nigam, M. Muralidharan, A. D. Domínguez-García, P. W. Sauer, and J. Kleissl, “Simulation of microgrid response with distributed controls and HIL tests for USCD microgrid,” Tech. Rep., 2018.
- [12] A. E. Fitzgerald, C. Kingsley, and S. D. Umans, *Electric Machinery*, 7th ed. McGraw-Hill, 2014.
- [13] D. Montenegro and R. C. Dugan, *OpenDSS PVSystem Element Model*. EPRI, March 2018, p. 1–10.
- [14] “Inverter performance test summaries.” [Online]. Available: https://www.gosolarcalifornia.ca.gov/equipment/inverter_tests/summaries/
- [15] Yingli Solar, “YGE 60 cell HSF smart datasheet.” [Online]. Available: http://www.yinglisolar.com/static/assets/uploads/products/downloads/DS_YGE60CELLSERIES2HSFSMART-29b_35mm_EU_EN_20180615_V04.pdf
- [16] “Solar resource data and tools.” [Online]. Available: <https://www.nrel.gov/grid/solar-resource/renewable-resource-data.html>
- [17] “Wind generation and total load in the BPA balancing authority.” [Online]. Available: <https://transmission.bpa.gov/Business/Operations/Wind/>
- [18] National Centers for Environmental Information, “Climate data online: Dataset discovery.” [Online]. Available: <https://www.ncdc.noaa.gov/cdo-web/datasets>
- [19] The Royal Academy of Engineering, “Wind turbine power calculations.” [Online]. Available: <https://www.raeng.org.uk/publications/other/23-wind-turbine>
- [20] J. V. Paatero and P. D. Lund, “A model for generating household electricity load profiles,” *International Journal of Energy Research*, vol. 30, no. 5, p. 273–290, 2006.
- [21] S. Kalogirou, *McEvoy’s Handbook of Photovoltaics: Fundamentals and Applications*, 3rd ed. Academic Press, an imprint of Elsevier, 2018.
- [22] Z. K. Pecanak, V. R. Disfani, M. J. Reno, and J. Kleissl, “Multiphase distribution feeder reduction,” *IEEE Transactions on Power Systems*, vol. 33, no. 2, p. 1320–1328, 2018.